

TIP AND POLISH: TEXT-IMAGE-PROTOTYPE GUIDED MULTI-MODAL GENERATION VIA COMMONALITY-DISCREPANCY MODELING AND REFINEMENT

Zhiyong Ma*, Jiahao Chen[†], Qingyuan Chuai[‡]

Zhengping Li

Cao Tu Li (Guangzhou) Technology Co., Ltd
Research and Development Department
Guangzhou, Guangdong, China

Hong Kong Baptist University
Faculty of Science
Kowloon, Hong Kong

ABSTRACT

Multi-modal generation struggles to ensure thematic coherence and style consistency. Semantically, existing methods suffer from cross-modal mismatch and lack explicit modeling of commonality and discrepancy. Methods that rely on fine-grained training fail to balance semantic precision with writing style consistency. These shortcomings lead to sub-optimal generation quality. To tackle these issues, we propose **TIPPo**, a simple yet effective framework with explicit input modeling and comprehensive optimization objectives. It extracts the input text and images via multi-modal encoder and adapters, then measures the visual prototype. **Textual**, **Image**, and **Prototype** signals are then fed to our proposed Dual Alignment Attention and Difference Operator modules before language model decoding. The proposed **PolishPPO** reinforces the style consistency, while the unsupervised contrastive learning during SFT mitigates inter-sample representation collapse. Experimental results demonstrate the promising performance of **TIPPo** in automatic evaluation and LLM-based criteria for creativity and semantic consistency.

Index Terms— Multi-modal generation, Prototype, TIPPo

1. INTRODUCTION

Synthesizing content from multi-modal input signals (e.g., topic and image), Multi-Modal Generation (MMG) enables applications like creative writing, image captioning, and story telling [1]. The core pursuit of this field is ensuring **thematic coherence** and **stylistic consistency** of the generated results.

For **thematic coherence** [2, 3], current methods face three semantic challenges: (1) cross-modal mismatch, (2) neglected measurement of intra-modal discrepancy, and (3) insufficient mining of both inter- and intra-modal commonality. To narrow the cross-modal semantic gaps, most MMG methods adopt pre-trained multi-modal encoder (MME) to extract features from inputs, and equip themselves with pre-trained

language model decoders for basic generation ability [4, 5]. Building upon this paradigm, existing methods directly inject textual and visual signals into downstream decoders [6, 7]. However, intra-modal semantic variations are ubiquitous and non-negligible, and such unregulated usage of inputs increases the risk of semantic drift from the core theme during generation. Concurrently, although multi-modal inputs contain rich semantic knowledge (e.g., associations within images, correlations between text and image), the simple integration fails to fully leverage such richness, instead leading to marginal improvements in MMG [8, 9]. Thus, we argue that explicit modeling of semantic discrepancy and commonality is critical to achieving thematic coherence.

For **stylistic consistency**, the optimization objective should be further associated with the literal and semantic meaning of the method’s overall output [10, 11]. In general, token-level training tasks like the Next Token Prediction (NTP) are widely used in MMG to ensure the semantic precision [8]. However, these fine-grained objectives lack an overview of writing style and struggle to maintain the stylistic unification throughout the entire output [12, 13]. Therefore, we contend that comprehensive objectives are crucial for polishing the quality of MMG.

To address aforementioned challenges, we propose TIPPo, a Text, Image, and visual Prototype-guided framework that explicitly models the semantic commonality and discrepancy, while reinforcing the generation quality with innovative PolishPPO and unsupervised contrastive learning. Specifically, with the prototype intuitively carrying intra-modal semantic commonality, two modal-aware adapters are used for downstream task adaptation. In addition, we design an Dual Alignment Attention module to augment image signals guided by inter- and intra-modal semantic commonality. Meanwhile, the Difference Operator is designed to model and highlight the intra-modal discrepancy, thus alleviating detail lost. Finally, the textual signal, enhanced image signals, and differential signal are concatenated and injected into the language model for decoding natural language results.

To improve the generation quality, we introduce PolishPPO to provide hierarchical supervision (literal-level and

*Zhiyong Ma performed the work while chasing its PhD at South China University of Technology

[†]Equal Contribution to Zhiyong Ma

[‡]Corresponding Author

article-semantic-level) that explicitly guides style consistency while preserving semantic precision, which is tough for the method supervised by fine-grained optimization objectives. Besides, the unsupervised contrast is used with supervised fine-tuning (SFT). It takes the prototype as the positive anchor of the image signal while setting the other samples within the same batch as the negative anchors, to learn and extract more discriminative features under semantic constrain, preventing the representation collapse.

Our key contributions are: (1) Proposing a MMG framework **TIPPo** that explicitly models semantic commonality/discrepancy to ensure thematic coherence, and integrates comprehensive optimization to enhance stylistic consistency; (2) Introducing PolishPPO and prototype-driven contrastive learning strategies to balance semantic precision with stylistic consistency and mitigate representation collapse.

2. PROPOSED METHOD

We propose TIPPo, a multimodal generation framework that captures inter-modal commonalities and intra-modal differences, with various training objectives, as shown in Fig.1. Firstly, the given text \mathcal{T} and N associated images $\mathcal{I} = \{\mathcal{I}_1, \dots, \mathcal{I}_N\}$, TIPPo extracts the corresponding signals by a frozen MME ϕ and trainable two adapters, π_T and π_V , where the textual signal $S^T = \pi_T(\phi(\mathcal{T}))$, the image signals $S^I = \{S_i^I = \pi_T^I(\phi(\mathcal{I}_i)) \mid i = 1, \dots, N\}$, and the prototype signal $S^P = \frac{1}{N} \sum_i^N S_i^I$. Leveraging S^T , S^I and S^P , the Dual Alignment Attention module augments each image signal, and the corresponding result S_i^A and S_A are as Eq.1-2. Then S^I and S^P are used to get the differential signal of i -th image S_i^D and the corresponding set S^D by the Difference Operator as Eq. 3-4. Finally, textual signal S^T , augmented signals S^A and differential signal S^D are concatenated to get the fusion signal $S^F = \{S_i^F = [S^T; S_i^A; S_i^D] \mid i = 1, 2, \dots, N\}$. The language model decoder $LM(\cdot)$ generate the result $y = LM(S^F)$. During training, we first conduct SFT with NTP and contrastive constrain (see Eq. 5) as: $\mathcal{L}_{SFT} = \mathcal{L}_{NTP} + \mathcal{L}_C$, then use PolishPPO to further optimize. Details are as follow.

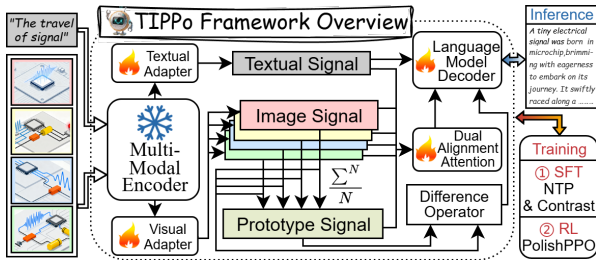


Fig. 1. The overview of TIPPo framework

2.1. Dual Alignment and Differential Signal

Existing methods demonstrated the effectiveness about the alignment process in capturing the semantic commonality [1, 6]. To leverage the inter- and intra-modal semantic commonality to enhance image signals, the Dual Alignment Attention (DAA) module is proposed. It builds the text-image alignment attention map and the prototype-image alignment attention map, where the first map tries to mine the inter-modal semantic commonality, while the second map focuses on measuring intra-modal semantic commonality. Two dual maps jointly enhance image signals for better MMG.

Specifically, it sets the textual query $Q^T = W^{TQ} \odot S^T$, prototype query $Q^P = W^{PQ} \odot S^P$, text-image key $K^T = \{K_i^T = W^{TIK} \odot S_i^I \mid i = 1, \dots, N\}$, prototype-image key $K^P = \{K_i^P = W^{PIK} \odot S_i^I \mid i = 1, \dots, N\}$ and visual values $V^I = \{V_i^I = W^V \odot S_i^I \mid i = 1, \dots, N\}$, where all the W^* are trainable parameters. Denoting $\sigma(\cdot)$ as the softmax operator, the augmented image signal S^A is constructed by:

$$S^A = \{S_i^A \mid i = 1, \dots, N\} \quad (1)$$

$$S_i^A = \left[\lambda_1 \cdot \sigma \left(\frac{Q^P K^P}{\sqrt{d_k}} \right) + \lambda_2 \cdot \sigma \left(\frac{Q^T K^T}{\sqrt{d_k}} \right) \right] V_i^I. \quad (2)$$

Notably, λ_1 and λ_2 in Eq. 2 are tied to the training stage, with $\lambda_1 = m/M$ and $\lambda_2 = 1 - \lambda_1$ (m : current step, M : total steps). This dual-weight scheduling balances learning generalizable prototype-guided semantics in the early phase and refining personalized inter-modal details as training advances, tackling the generality-specificity trade-off in MMG. As λ_1 rises, it gradually emphasizes prototype-grounded semantic detail augmentation for images, while λ_2 sustains explicit inter-modal commonality modeling and attention to personalized fine-grained details.

In addition, to fully exploit the unique visual detail, we propose the Difference Operator (DO). Existing methods predominantly focus on capturing commonalities (e.g., shared semantic concepts) [9, 7]. However, intra-modal discrepancies are also critical for generating fine-grained content. For instance, in scenes with multiple similar objects, intra-modal discrepancies in image features like subtle shape or texture variations are intuitively crucial for distinguishing each object precisely. Thus, the Difference Operator targets this unexploited dimension by measuring and refining intra-modal differential information to obtain the differential signal S^D , where π_D represents a trainable linear layer:

$$S^D = \{S_i^D \mid i = 1, \dots, N\} \quad (3)$$

$$S_i^D = (S_i^I - S^P) + \pi_D(S_i^I - S^P). \quad (4)$$

Notably, the residual design in Eq. 4 enables flexible control over the strength of S^D . When the differential information is not beneficial or even detrimental to the downstream task (e.g., noisy details), the π_D can adaptively reduce the influence. This mechanism allows our framework to neglect or

even degrade inappropriate differential information, ensuring that only useful differential information contributes to the final generation, enhancing the robustness and adaptability.

2.2. Contrastive Constraint and PolishPPO

To mitigate representation collapse we design an unsupervised contrastive constraint in SFT that brings the representation of each image closer to its corresponding prototype while distinguishing from others. In other words, we take the prototype signal as the positive anchor of each image while taking the other images as the negative set in InfoNCE [14]:

$$\mathcal{L}_C = -\frac{1}{N} \sum_{i=1}^N \log \left(\frac{\exp(\cos(S_i^I, S_i^P))}{\sum_{j=1}^N \exp(\cos(S_i^I, S_j^I))} \right). \quad (5)$$

In cases where only one corresponding image exists (like one image pair for one or no textual instruction in image captioning), the prototype can be measured as the average of the image signals from the same batch, and negative samples are the other images within the same batch.

In addition, the fine-grained optimization objective is hard to explicitly guide style consistency while preserving semantic precision. PolishPPO is proposed to address this dilemma by providing literal-level and article-semantic-level supervision. It adjusts the **cumulative discounted return** G_m , and the **normalized advantage estimation** \hat{A} in PPO [11]:

$$\hat{A} := \frac{G_m - \mu_m}{\delta_m + \epsilon}, \quad \epsilon := 1e - 8, \quad (6)$$

where μ_m and δ_m are the expectation and variance over the last m iterations. $G_m = \gamma^m R_{literal} + \gamma^{M-m} R_{semantic}$, where γ is a scalar hyperparameter set as 0.95, with its exponents determined by current and total training steps (m and M). Denote the ground-truth of the generation result y as Y . We obtain their embedding emd_Y and emd_y via GLM [15]. Denotes the $LD(\cdot, \cdot)$ as the Levenshtein distance operator, and \cos as the cosine operator same in Eq. 5 Then literal-level reward $R_{literal}$ and the semantic-level reward $R_{semantic}$ used in G_m are respectively obtained as:

$$R_{literal} = 1 - LD(Y, y), \quad (7)$$

$$R_{semantic} = \cos(emd_Y, emd_y). \quad (8)$$

3. EXPERIMENTS

3.1. Experimental settings

TIPPO is evaluated on two MMG datasets. The first is *ArtMuse* [10], a creative writing dataset with 100 articles, each contains a textual title, 3–5 associated images, and a reference result. The second is *COCO-CN* [16], a mage captioning dataset in Chinese (built on *MS-COCO*) with 22k manual sentences and 5k translated sentences. We adopt two

test beds upon automatic evaluation and LLM-based criteria measure the generation quality. For automatic evaluation, we employ metrics including Rouge-L, METEOR, CIDEr, and BertScore following [17, 18]. Considering the limitations of these metrics in holistically, we further use LLM-based criteria for creativity and semantic consistency following [10], which assesses results from 10 perspectives. We initialize the MME and the Language Model Decoder from *OFA-Sys/chinese-clip-vit-base-patch16* and *langboat/mengzi-t5-base*. During SFT, TIPPO trains 50K iterations with learning rate $\eta_{SFT} = 5e - 5$ verified from {3e-5, 4e-5, 5e-5, 6e-5, 7e-5}. The PolishPPO executes 20K iterations with $\eta_{PPO} = 1e - 5$ verified from {6e-6, 9e-6, 1e-5, 3e-5, 5e-5}.

3.2. Experimental Results

Overall, TIPPO achieves promising performance in different aspects. Specifically, as shown in Table 1, TIPPO shows decent performance within 3 metrics on *ArtMUSE*, where METEOR, ROUGE-L and BertScore respectively increase 4.56, 8.1 and 0.06 relative to the second best method.

Table 1. Automatic evaluation on *ArtMUSE*. The best and the second results are in **bold** and underline respectively.

| methods | METEOR | ROUGE-L | BertScore |
|-----------------|--------------|--------------|-------------|
| mm-cot [7] | 1.64 | 12.02 | 0.43 |
| mPLUG-Owl [4] | 4.48 | 14.21 | 0.63 |
| LaDic [19] | 7.31 | 12.13 | 0.55 |
| DOC [20] | 1.99 | 8.02 | 0.65 |
| GLM-4V [15] | 1.41 | 9.34 | 0.66 |
| Qwen2.5-v1 [21] | 1.28 | 9.37 | 0.65 |
| GPT-4o [22] | 3.53 | 9.41 | 0.66 |
| FlexMUSE [10] | <u>23.32</u> | <u>30.18</u> | <u>0.71</u> |
| TIPPO | 27.88 | 38.28 | 0.77 |

Besides, TIPPO achieves the highest performance on *COCO-CN* in METEOR and ROUGE-L, exceeding HARN [8] by 21.22 and 3.96, respectively, as shown in Table 2. However, its CIDEr remains lower than HARN. This performance gap might be caused by CIDEr prioritizes the coverage of high-frequency key words in reference texts, while TIPPO focuses more on the overall semantic consistency and logical coherence of generated descriptions rather than deliberately matching such high-frequency local details.

As shown in Fig. 3, TIPPO demonstrates promising results in LLM evaluation. Specifically, TIPPO outperforms all comparison methods in CC^f , CC^a , CO^f , and CO^a (defined in [10]), reflecting its superiority in addressing thematic coherence issues. The performance about SC^f and SC^a (also defined in [10]) highlight the effectiveness in solving the stylistic consistency challenge.

| | Paradigm | | | | Paradigm | | | | Paradigm | | | |
|--------|------------|-------|-----------|------------------------|------------|-------|-----------|------------------------|------------|------|-----------|------------------------|
| | METEOR | NTP | +Contrast | +Contrast & +PolishPPO | ROUGE-L | NTP | +Contrast | +Contrast & +PolishPPO | BertScore | NTP | +Contrast | +Contrast & +PolishPPO |
| Module | TIP | 17.21 | 21.56 | 24.12 | TIP | 30.35 | 32.71 | 35.3 | TIP | 0.66 | 0.68 | 0.69 |
| | +DAA | 18.85 | 23.72 | 26.95 | +DAA | 31.92 | 34.45 | 37.1 | +DAA | 0.7 | 0.71 | 0.72 |
| | +DAA & +DO | 19.33 | 25.86 | 27.88 | +DAA & +DO | 32.41 | 35.98 | 38.28 | +DAA & +DO | 0.73 | 0.75 | 0.77 |

Fig. 2. Effectiveness of individual modules or methods in TIPPo evaluated by automatic metric on ArtMUSE.

3.3. Ablation study

We record the ablation results in Fig. 2, evaluating the contributions of DAA, DO and training strategies. We denotes TIP as a baseline method which ablate the DAA and DO from TIPPo. Module-wise (vertical) comparisons reveal consistent performance enhancements with the incremental integration of components across all optimization paradigms. Paradigm-wise (horizontal) comparisons demonstrate progressive enhancements from advanced optimization objectives. These results validate the contribution of each design in TIPPo.

Table 2. Automatic evaluation on *COCO-CN*. The best and the second results are in **bold** and underline respectively.

| methods | METEOR | ROUGE-L | CIDEr |
|------------------|--------------|--------------|--------------|
| Meng et al. [23] | 12.1 | 22.8 | 34.9 |
| Ukyo et al. [24] | 12.8 | 23.4 | 19.7 |
| HARN [8] | <u>29</u> | <u>50.3</u> | 89.8 |
| TIPPo | 50.22 | 54.26 | <u>59.35</u> |

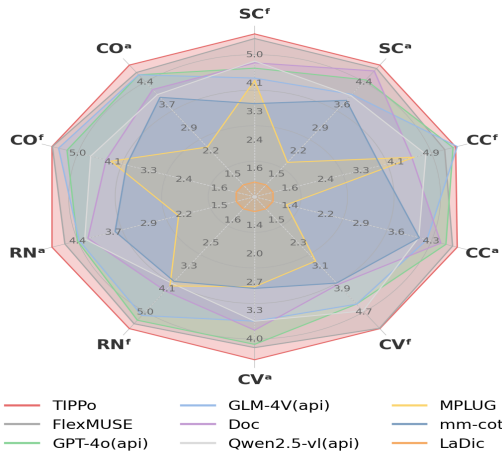


Fig. 3. LLM evaluation of different methods on ArtMUSE.

To further validate the effectiveness of PolishPPO, we conducted additional verifications with different optimization objectives using the TIP without prototype input, as shown in Table 3. When only NTP is employed, the performance in three criterias is almost at the peak once the iteration reaches

Table 3. Comparison about the of optimization objectives.

| ArtMuse | Iterations | METEOR | ROUGE-L | BertScore |
|----------------|------------|--------|---------|-----------|
| PolishPPO Only | 20k | 3.26 | 4.57 | 0.57 |
| | 50k | 5.64 | 8.97 | 0.58 |
| | 70k | 6.21 | 11.24 | 0.60 |
| | 80k | 6.06 | 11.14 | 0.60 |
| | 90k | 6.11 | 11.17 | 0.59 |
| NTP Only | 30k | 8.34 | 15.39 | 0.62 |
| | 40k | 8.77 | 16.98 | 0.62 |
| | 50k | 10.82 | 18.43 | 0.62 |
| | 60k | 10.23 | 18.14 | 0.62 |
| | 70k | 9.98 | 16.24 | 0.61 |
| Both | 50+20k | 17.53 | 27.89 | 0.64 |

50k. In comparison, continuing optimization with PolishPPO following 50k steps of NTP (last line records) show effective improvement in model performance. Moreover, we also set up several test beds that training the baseline only with PolishPPO. As expected, the performance of the baseline gradually improved with iteration, and approached the optimal result with 70k iterations. The above validations indicate that PolishPPO, as a complementary refinement step to SFT (NTP), can effectively improve the overall quality of MMG.

4. CONCLUSION

In this work, we propose a text-image-prototype guided multi-modal generation framework, namely TIPPo. To ensure thematic coherence, TIPPo integrates the Dual Alignment Attention to augment image signals guided by inter- and intra-modal semantic commonality. Additionally, a Difference Operator is integrated to model and highlight the intra-modal discrepancy, thus alleviating detail lost. Furthermore, to improve the generation quality, we introduce PolishPPO to provide hierarchical supervision that explicitly guides style consistency. Enabled by its well-designed modules and training strategies, TIPPo achieves promising performance on ArtMuse and COCO-CN datasets. Future work will explore extending TIPPo to more complex multi-modal scenarios (e.g., video-text generation) and optimizing its efficiency for real-time applications.

5. REFERENCES

- [1] Fatemeh Nazarieh, Zhenhua Feng, Muhammad Awais, Wenwu Wang, and Josef Kittler, “A survey of cross-modal visual content generation,” *IEEE Transactions on Circuits and Systems for Video Technology*, vol. 34, pp. 6814–6832, Aug. 2024.
- [2] Dizhan Xue, Shengsheng Qian, Quan Fang, and Changsheng Xu, “Mmt: Image-guided story ending generation with multimodal memory transformer,” in *ACM MM 2022*, Lisboa Portugal, Oct. 2022, p. 750–758, ACM.
- [3] Xiaoyong Liu, Jiahao Chen, Chunlin Xu, Zhiguo Du, Weiqi Chen, and Huihui Li, “Sentiment-enhanced triplet region detection framework for aspect sentiment triplet extraction,” *Neurocomputing*, vol. 644, pp. 130392, 2025.
- [4] Qinghao Ye, Haiyang Xu, Guohai Xu, et al., “mplug-owl: Modularization empowers large language models with multimodality,” *arXiv preprint 22304.14178*, 2024.
- [5] Yayun Qi, Hongxi Li, Yiqi Song, Xinxiao Wu, and Jiebo Luo, “How vision-language tasks benefit from large pre-trained models: A survey,” *arXiv preprint 2412.08158*, 2024.
- [6] Li Yang, Zhiding Xiao, Wenxin Huang, and Xian Zhong, “Storyllava: Enhancing visual storytelling with multi-modal large language models,” in *COLING 2025*, Abu Dhabi, UAE, Jan. 2025, p. 3936–3951, ACL.
- [7] Zhuosheng Zhang, Aston Zhang, Mu Li, Hai Zhao, George Karypis, and Alex Smola, “Multimodal chain-of-thought reasoning in language models,” *arXiv preprint 2302.00923*, 2023.
- [8] Zijie Song, Zhenzhen Hu, Yuanen Zhou, Ye Zhao, Richang Hong, and Meng Wang, “Embedded heterogeneous attention transformer for cross-lingual image captioning,” *IEEE Transactions on Multimedia*, vol. 26, pp. 9008–9020, 2024.
- [9] Fengxiang Bie, Yibo Yang, Zhongzhu Zhou, et al., “Renaissance: A survey into ai text-to-image generation in the era of large model,” *IEEE Transactions on Pattern Analysis and Machine Intelligence*, vol. 47, pp. 2212–2231, Mar. 2025.
- [10] Jiahao Chen, Zhiyong Ma, Wenbiao Du, and Qingyuan Chuai, “Flexmuse: Multimodal unification and semantics enhancement framework with flexible interaction for creative writing,” *arXiv preprint 2508.16230*, 2025.
- [11] John Schulman, Filip Wolski, Prafulla Dhariwal, Alec Radford, and Oleg Klimov, “Proximal policy optimization algorithms,” Aug. 2017.
- [12] Rafael Rafailov, Archit Sharma, Eric Mitchell, Stefano Ermon, et al., “Direct preference optimization: Your language model is secretly a reward model,” July 2024.
- [13] Jie Zhao, Ziyu Guan, Cai Xu, Wei Zhao, and Yue Jiang, “SC2: Towards enhancing content preservation and style consistency in long text style transfer,” Aug. 2024, Association for Computational Linguistics.
- [14] Ting Chen, Simon Kornblith, Mohammad Norouzi, and Geoffrey Hinton, “A simple framework for contrastive learning of visual representations,” in *International conference on machine learning*. PmlR, 2020, pp. 1597–1607.
- [15] Team GLM, Aohan Zeng, Bin Xu, et al., “Chatglm: A family of large language models from glm-130b to glm-4 all tools,” *arXiv preprint 2406.12793*, 2024.
- [16] Xirong Li, Chaoxi Xu, Xiaoxu Wang, Weiyu Lan, et al., “Coco-cn for cross-lingual image tagging, captioning, and retrieval,” *IEEE Transactions on Multimedia*, vol. 21, pp. 2347–2360, 2019.
- [17] Xin Li, Chunping Liu, and Yi Ji, “Associative learning network for coherent visual storytelling,” in *ICASSP 2023*. IEEE, 2023, pp. 1–5.
- [18] Jiaqi Su, Weiran Chen, Yi Ji, and Chunping Liu, “Global cascading network for topic enhanced visual storytelling,” in *ICASSP 2024*. IEEE, 2024, pp. 2845–2849.
- [19] Yuchi Wang, Shuhuai Ren, Rundong Gao, Linli Yao, et al., “Ladic: Are diffusion models really inferior to autoregressive counterparts for image-to-text generation?,” *arXiv preprint 2404.10763*, 2024.
- [20] Kevin Yang, Dan Klein, Nanyun Peng, and Yuandong Tian, “DOC: Improving long story coherence with detailed outline control,” in *ACL 2023*, Toronto, Canada.
- [21] Shuai Bai, Keqin Chen, Xuejing Liu, Jialin Wang, et al., “Qwen2.5-vl technical report,” *arXiv preprint 2502.13923*, 2025.
- [22] OpenAI, Aaron Hurst, Adam Lerer, Adam P. Goucher, et al., “Gpt-4o system card,” *arXiv preprint 2410.21276*, 2024.
- [23] Zihang Meng, David Yang, Xuefei Cao, Ashish Shah, and Ser-Nam Lim, “Object-centric unsupervised image captioning,” *arXiv preprint 2112.00969*, 2022.
- [24] Ukyo Honda, Yoshitaka Ushiku, Atsushi Hashimoto, Taro Watanabe, and Yuji Matsumoto, “Removing word-level spurious alignment between images and pseudo-captions in unsupervised image captioning,” in *EACL 2021*, 2021, pp. 3692–3702.